ELSEVIER

International Journal of Solids and Structures 41 (2004) 947–964

INTERNATIONAL JOURNAL OF SOLIDS and STRUCTURES

www.elsevier.com/locate/ijsolstr

3D free vibration analysis of a functionally graded piezoelectric hollow cylinder filled with compressible fluid

W.Q. Chen *, Z.G. Bian, C.F. Lv, H.J. Ding

Department of Civil Engineering, Zhejiang University, Zheda Road 38, Hangzhou 310027, PR China

Received 15 April 2003; received in revised form 18 August 2003

Abstract

The free vibration of an arbitrarily thick orthotropic piezoelectric hollow cylinder with a functionally graded property along the thickness direction and filled with a non-viscous compressible fluid medium is investigated. The analysis is directly based on the three-dimensional exact equations of piezoelasticity using the so-called state space formulations. The original functionally graded shell is approximated by a laminate model, of which the solution will gradually approach the exact one when the number of layers increases. The effect of internal fluid can be taken into consideration by imposing a relation between the fluid pressure and the radial displacement at the interface. Analytical frequency equations are derived for different electrical boundary conditions at two cylindrical surfaces. As particular cases, free vibration of multi-layered piezoelectric hollow cylinder and wave propagation in infinite homogeneous cylinder are studied. Numerical comparison with available results is made and dispersion curves predicted from the present three-dimensional analysis are given. Numerical examples are further performed to investigate the effects of various parameters on the natural frequencies.
© 2003 Elsevier Ltd. All rights reserved.

Keywords: Free vibration; Functionally graded piezoelectric material; State equation; Approximate laminate model; Hollow cylinder; Fluid-structure interaction

1. Introduction

Since the piezoelectric phenomenon was first discovered by Pierre and Paul-Jacques Curie in 1880, piezoelectric materials have attracted many attentions in both theoretical and engineering science and lots of efforts have been made on the quality and variety of artificial piezoelectric materials, which have been widely used to manufacture various sensors, conductors, actuators, etc. (Moulson and Herbert, 1990; Morita et al., 1995; Uchino, 1996). In fact, piezoelectric materials have become one of the most widely used smart or intelligent materials nowadays (Tzou and Anderson, 1992; Galassi et al., 2000). Experimental evidence has also indicated that bones could be modeled as a piezoelectric cylindrical shell, which is in fact inhomogeneous (Saha and Williams, 1996).

* Corresponding author. Tel.: +86-571-879-52284; fax: +86-571-879-52165.
E-mail addresses: chenwq@ccea.zju.edu.cn, chenwq@rocketmail.com (W.Q. Chen).

0020-7683/$ - see front matter © 2003 Elsevier Ltd. All rights reserved.
doi:10.1016/j.ijsolstr.2003.09.036

In recent years, the concept of functionally graded materials (FGMs) has been further extended into piezoelectric materials to improve the lifetime and reliability of advanced piezoelectric structures (Zhu et al., 1995; Wu et al., 1996; Sakamura et al., 2000; Yamada et al., 2001; Ballato et al., 2001; Takahashi et al., 2002). Smart structures or elements made of these so-called functionally graded piezoelectric materials (FGPMs) are usually superior to the conventional laminated piezoelectric ones (such as the bimorphs) because no discernible internal seams or boundaries exist and no internal stress peaks are caused when voltage is applied and thus failure from interfacial debonding or from stress concentration can be avoided (Wu et al., 1996; Li and Weng, 2002). Moreover, the performance of conventional homogeneous piezoelectric structures can be improved by using the concept of FGM. For example, Takagi et al. (2002) applied the modified classical lamination theory and the finite element method to optimize compositional profile of functionally graded PZT/Pt piezoelectric bimorph actuator that will give a larger deflection and smaller stress. To design advanced smart structures, it is necessary to thoroughly understand the static and dynamic behaviors of FGPM structures in complex environments. The focus of this paper is to study the dynamic behavior of fluid-filled FGPM cylindrical shells. The conventional homogeneous or laminated piezoelectric cylindrical shells coupled with fluids are encountered in various applications like fluid control valve, ink jet printer, and submarine ultrasonic transducers (Bugdayci et al., 1983; Grosh et al., 1998).

In this paper, the coupled vibration of an inhomogeneous orthotropic piezoelectric hollow cylinder filled with internal compressible fluid is studied directly based on the three-dimensional equations of piezoelasticity. The cylinder is assumed to have a functionally graded property along the thickness direction (radial direction) and is polarized in the axial direction. The state-space method is employed, which has the particular superiority to study laminated plates and shells (Fan, 1996; Chen and Ding, 2001). We further employ a laminate model (Fan and Zhang, 1992; Liu and Tani, 1991; Tanigawa, 1995; Chen and Ding, 2000) to approximate the FGPM hollow cylinder. It is obvious that the larger the number of layers involved is, the accurate the model will be. By employing the continuity conditions of state variables between adjacent layers, recurrence formulas are established. The frequency equation is then deduced for a simply supported FGPM hollow cylinder filled with a compressible, non-viscous fluid medium with different electrical boundary conditions imposed on the two cylindrical surfaces. The one for an infinite homogeneous piezoelectric hollow cylinder is considered as a particular case and numerical comparison is made with available results. The effects of some related parameters on natural frequencies are also discussed. The present method allows us to consider arbitrary variations of material properties along the thickness direction. The 3D solution obtained here can provide a useful means of comparison in the development of simplified shell theories of non-homogeneous FGPM cylindrical shells coupled with surrounding media.

2. Brief literature survey

Generally, the elastic deformation and electric field of piezoelectric materials are coupled, which makes the governing equations very complex. The classical theories for plates and shells are not so suitable here because the electric potential through the thickness is no longer linear so that higher-order representations should be adopted (Rogacheva, 1994). Especially, these theories usually become inaccurate and even invalid when the plate or shell becomes thicker, just as in the elastic case. Thus, in the most recent decade, much investigation on piezoelectric cylindrical shells was to obtain 3D solutions (Ding et al., 1997a; Kapuria et al., 1997; Chen and Shen, 1998). Xu and Noor (1996) analyzed the thermal piezoelastic response of a layered piezoelectric material (LPM) cylindrical shell employing the transfer matrix method. Xu et al. (1997) further studied the free vibrations of a thermal LPM cylindrical shell with initial stresses. Zhou et al. (1999) established a state equation with constant coefficients by introducing a small parameter and considered the static response of an LPM cylindrical shell. The polarized direction of piezoelectric cylindrical shell in the

above-mentioned studies is considered to be along the radial direction. Wang (2001) investigated the one polarized in the axial direction, but using the membrane shell theory.

Coupled vibrations of fluid-filled cylindrical shells were first considered by Junger and Mass (1952), which was followed by Jain (1974), who discussed the free vibrations of orthotropic cylindrical shells filled partially or completely with an incompressible, non-viscous fluid using a shear shell theory. Recently, based on Love's shell theory, Zhang et al. (2001) expressed the displacements of the shell as the form of wave propagation to analyze the coupled vibrations of fluid-filled cylindrical shell. There are also several three-dimensional analyses of fluid-filled cylindrical shells. Chen et al. (1997) used the Frobenius power series method to investigate the free vibrations of fluid-filled orthotropic cylindrical shells. Chen and Ding (1999) employed a displacement separation formula to simplify the basic equations of a transversely isotropic medium and considered the vibration of a fluid-filled transversely isotropic cylindrical shell. The coupled analysis of piezoelectric cylindrical shells has also attracted particular interests, since it is essential for their frequent encounters in some engineering applications (Babaev and Savin, 1988; Babaev et al., 1990; Shulga and Melnik, 1996; Ding et al., 1997a). The 3D coupled free vibration of a fluid-filled piezoelectric hollow sphere was considered by Chen et al. (2001) employing the Frobenius power series method.

The concept of FGM was first introduced by a group of Japanese scientists to address the needs of aggressive environment of thermal shock (Yamanouchi et al., 1990). Since then, FGMs have received more and more attention. On the macroscopic scale, FGMs are anisotropic, inhomogeneous and possess spatially continuous mechanical properties. Heretofore, a lot of works on the FGM cylindrical shells have been carried out. For example, employing Love's shell theory and Rayleigh–Ritz method, Loy et al. (1999) obtained the natural frequencies of a simply supported FGM cylindrical shell. Applying the same method but a modified expression of spatial displacement fields, Pradhan et al. (2000) further studied the vibration characteristics of the FGM cylindrical shell under various boundary conditions. Tarn (2001) obtained some exact thermoelastic solutions of an anisotropic cylinder with a particular functionally graded property. Han et al. (2001) presented a hybrid numerical method to investigate transient waves in a cylinder made of FGM; the cylinder was divided into some cylindrical elements that the material properties were approximated with piecewise linear functions. It is noted here that as in the early of 1990s, Liu and Tani have investigated the wave propagation in FGPM plates of which the material properties are approximated by piecewise linear functions (Liu and Tani, 1991, 1992). Chen and Ding (2000, 2002) employed the state-space approach to analyze the bending and free vibration problems of FGPM plates using a laminate model, for which material properties were treated as piecewise constants. Recently, Wu et al. (2002) introduced a high-order shell theory and examined the electromechanical behavior of graded piezoelectric shells. Wu et al. (2004) obtained an exact solution for a piezothermoelastic cylindrical shell with radial inhomogeneity acting as a smart device subjected to thermal and mechanical loadings.

3. State equation

In cylindrical coordinates (r, ϕ, z), Fig. 1, the basic equations of orthotropic piezoelectric materials polarized in the axial direction are (Ding and Chen, 2001)

Generalized geometric equations:

$$\begin{aligned}
&\gamma_{rr} = \frac{\partial u_r}{\partial r}, \quad \gamma_{\phi\phi} = \frac{\partial u_\phi}{r\partial\phi} + \frac{u_r}{r}, \quad \gamma_{zz} = \frac{\partial u_z}{\partial z},\\
&\gamma_{r\phi} = \frac{1}{2}\left(\frac{\partial u_r}{r\partial\phi} + \frac{\partial u_\phi}{\partial r} - \frac{u_\phi}{r}\right), \quad \gamma_{\phi z} = \frac{1}{2}\left(\frac{\partial u_\phi}{\partial z} + \frac{\partial u_z}{r\partial\phi}\right), \quad \gamma_{zr} = \frac{1}{2}\left(\frac{\partial u_z}{\partial r} + \frac{\partial u_r}{\partial z}\right),\\
&E_r = -\frac{\partial \Phi}{\partial r}, \quad E_\phi = -\frac{\partial \Phi}{r\partial\phi}, \quad E_z = -\frac{\partial \Phi}{\partial z}.
\end{aligned} \tag{1}$$

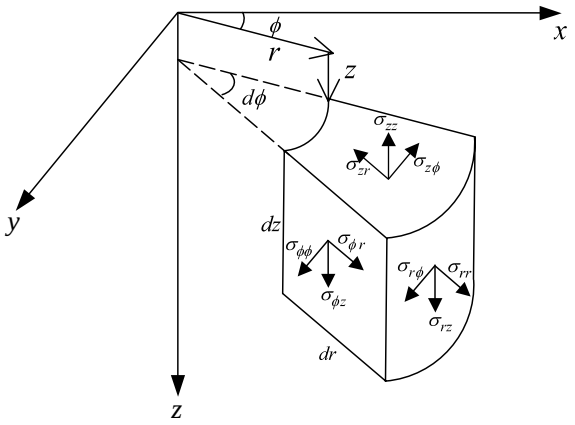

Fig. 1. Cylindrical coordinates and stresses.

Generalized constitutive relations:

$$\begin{aligned}
&\sigma_{rr} = c_{11}\gamma_{rr} + c_{12}\gamma_{\phi\phi} + c_{13}\gamma_{zz} - e_{31}E_z, \quad \sigma_{r\phi} = 2c_{66}\gamma_{r\phi},\\
&\sigma_{\phi\phi} = c_{12}\gamma_{rr} + c_{22}\gamma_{\phi\phi} + c_{23}\gamma_{zz} - e_{32}E_z, \quad \sigma_{\phi z} = 2c_{44}\gamma_{\phi z} - e_{24}E_\phi,\\
&\sigma_{zz} = c_{13}\gamma_{rr} + c_{23}\gamma_{\phi\phi} + c_{33}\gamma_{zz} - e_{33}E_z, \quad \sigma_{zr} = 2c_{55}\gamma_{zr} - e_{15}E_r,\\
&D_\phi = 2e_{24}\gamma_{\phi z} + \varepsilon_{22}E_\phi, \quad D_r = 2e_{15}\gamma_{zr} + \varepsilon_{11}E_r, \quad D_z = e_{31}\gamma_{rr} + e_{32}\gamma_{\phi\phi} + e_{33}\gamma_{zz} + \varepsilon_{33}E_z.
\end{aligned} \tag{2}$$

Governing equations:

$$\begin{aligned}
&\frac{\partial\sigma_{zr}}{\partial r} + \frac{\partial\sigma_{\phi z}}{r\partial\phi} + \frac{\partial\sigma_{zz}}{\partial z} + \frac{\sigma_{zr}}{r} + f_z = \rho\frac{\partial^2 u_z}{\partial t^2},\\
&\frac{\partial\sigma_{r\phi}}{\partial r} + \frac{\partial\sigma_{\phi\phi}}{r\partial\phi} + \frac{\partial\sigma_{\phi z}}{\partial z} + \frac{2\sigma_{r\phi}}{r} + f_\phi = \rho\frac{\partial^2 u_\phi}{\partial t^2},\\
&\frac{\partial\sigma_{rr}}{\partial r} + \frac{\partial\sigma_{r\phi}}{r\partial\phi} + \frac{\partial\sigma_{zr}}{\partial z} + \frac{\sigma_{rr} - \sigma_{\phi\phi}}{r} + f_r = \rho\frac{\partial^2 u_r}{\partial t^2},\\
&\frac{\partial D_r}{\partial r} + \frac{\partial D_\phi}{r\partial\phi} + \frac{\partial D_z}{\partial z} + \frac{D_r}{r} = \rho_{\mathrm{f}},
\end{aligned} \tag{3}$$

where Φ, E_ℓ and D_ℓ ($\ell = r, \phi, z$) are the electric potential, electric intensity and electric displacements, respectively, f_ℓ ($\ell = r, \phi, z$) and ρ_{f} are components of body force and the free charge density, respectively, and c_{ij}, ε_{ij} and e_{ij} are the elastic, dielectric and piezoelectric constants, respectively. For a functionally graded piezoelectric cylindrical shell that is inhomogeneous along the radial direction, all material constants including the mass density are functions of the radial variable r.

Following a routine way (Fan and Zhang, 1992; Chen and Ding, 2000; Ding and Chen, 2001), the state equation can be readily derived from Eqs. (1) to (3). Here we just give the form in absence of body force and free charge density:

$$\frac{\partial}{\partial r}\mathbf{Y} = \mathbf{M}\mathbf{Y}, \tag{4}$$

where $\mathbf{Y} = [u_z, u_\phi, \sigma_{rr}, D_r, \sigma_{zr}, \sigma_{r\phi}, u_r, \Phi]^{\mathrm{T}}$ is the state vector and $\mathbf{M}$ is an eighth-order operator matrix, which is given in Appendix A. Eq. (4) was derived for a homogeneous piezoelectric cylindrical shell (Ding and

Chen, 2001), however, it is also valid for the one considered here that is inhomogeneous along the radial direction.

4. Free vibration of a fluid-filled FGPM hollow cylinder

Consider a simply supported FGPM hollow cylinder of length L, inner radius R and thickness h, Fig. 2. The state vector $\mathbf{Y}$ can be expanded as

$$\mathbf{Y} = \begin{Bmatrix} u_z \\ u_\phi \\ \sigma_{rr} \\ D_r \\ \sigma_{zr} \\ \sigma_{r\phi} \\ u_r \\ \Phi \end{Bmatrix} = \sum_{m=0}^{\infty}\sum_{n=0}^{\infty} \begin{Bmatrix} R\bar{u}_z(\eta)\cos(m\pi\zeta)\cos(n\phi) \\ R\bar{u}_\phi(\eta)\sin(m\pi\zeta)\sin(n\phi) \\ c_{44}^1\bar{\sigma}_{rr}(\eta)\sin(m\pi\zeta)\cos(n\phi) \\ \sqrt{c_{44}^1\varepsilon_{33}^1}\overline{D}_r(\eta)\cos(m\pi\zeta)\cos(n\phi) \\ c_{44}^1\bar{\sigma}_{zr}(\eta)\cos(m\pi\zeta)\cos(n\phi) \\ c_{44}^1\bar{\sigma}_{r\phi}(\eta)\sin(m\pi\zeta)\sin(n\phi) \\ R\bar{u}_r(\eta)\sin(m\pi\zeta)\cos(n\phi) \\ R\sqrt{c_{44}^1/\varepsilon_{33}^1}\overline{\Phi}(\eta)\cos(m\pi\zeta)\cos(n\phi) \end{Bmatrix} e^{i\omega t}, \tag{5}$$

where $\eta = r/R$, $\zeta = z/L$, m and n are integers and ω is the circular frequency. c_{44}^1 represents the value of c_{44} at the outer cylindrical surface $r = R + h$. It is immediately seen that the solutions given in Eq. (5) satisfy the simply supported mechanical conditions, i.e. $u_r = u_\phi = \sigma_{zz} = 0$ at $z = 0$ and L (Soldatos and Hadhgeorgiou, 1990; Ding et al., 1997b). Besides, the electric condition ($D_z = 0$ at $z = 0$ and L) is known as the open-circuit condition or insulated condition.

Substituting Eq. (5) into Eq. (4), and utilizing the orthogonality of trigonometric functions, one can obtain for an arbitrary couple of (m, n):

$$\frac{\mathrm{d}\mathbf{V}}{\mathrm{d}\eta} = \mathbf{D}\mathbf{V}, \tag{6}$$

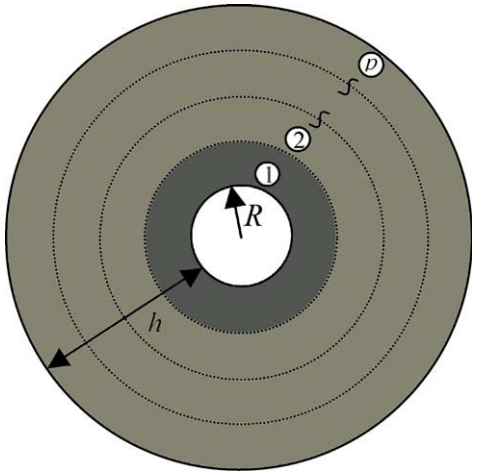

Fig. 2. Cylindrical shell section.

where $\mathbf{V} = [\bar{u}_z, \bar{u}_\phi, \bar{\sigma}_{rr}, \overline{D}_r, \bar{\sigma}_{zr}, \bar{\sigma}_{r\phi}, \bar{u}_r, \overline{\Phi}]^{\mathrm{T}}$. Denoting

$$
\begin{aligned}
&Rm\pi/L = \lambda, \quad R^2\omega^2\rho^1/c_{44}^1 = \Omega^2, \quad c_{12}c_{13}/(c_{11}c_{44}^1) - c_{23}/c_{44}^1 = d_1,\\
&e_{33}\Big/\sqrt{c_{44}^1\varepsilon_{33}^1} - c_{13}e_{31}\Big/\left(c_{11}\sqrt{c_{44}^1\varepsilon_{33}^1}\right) = d_2,\\
&e_{32}\Big/\sqrt{c_{44}^1\varepsilon_{33}^1} - c_{12}e_{31}\Big/\left(c_{11}\sqrt{c_{44}^1\varepsilon_{33}^1}\right) = d_4,\\
&c_{12}^2/(c_{11}c_{44}^1) - c_{22}/c_{44}^1 = d_3, \quad \varepsilon_{33}/\varepsilon_{33}^1 + e_{31}^2/(c_{11}\varepsilon_{33}^1) = d_5, \quad c_{13}^2/(c_{11}c_{44}^1) - c_{33}/c_{44}^1 = d_6,
\end{aligned}
\tag{7}
$$

the coefficient matrix $\mathbf{D}$ is expressed as

$$
\mathbf{D} = \begin{bmatrix} \mathbf{D}_{11} & \mathbf{D}_{12} \\ \mathbf{D}_{21} & \mathbf{D}_{22} \end{bmatrix}, \tag{8}
$$

where

$$
\mathbf{D}_{11} = \begin{bmatrix}
0 & 0 & 0 & e_{15}\sqrt{c_{44}^1\varepsilon_{33}^1}/(c_{55}\varepsilon_{11} + e_{15}^2) \\
0 & 1/\eta & 0 & 0 \\
d_1\lambda/\eta & -d_3 n/\eta^2 & (c_{12}/c_{11} - 1)/\eta & 0 \\
e_{24}n^2/(\eta^2\sqrt{c_{44}^1\varepsilon_{33}^1}) + d_2\lambda^2 & -(e_{24}/\sqrt{c_{44}^1\varepsilon_{33}^1} + d_4)n\lambda/\eta & -e_{31}\lambda\sqrt{c_{44}^1}/(c_{11}\sqrt{\varepsilon_{33}^1}) & -1/\eta
\end{bmatrix},
$$

$$
\mathbf{D}_{12} = \begin{bmatrix}
c_{44}^1\varepsilon_{11}/(c_{55}\varepsilon_{11} + e_{15}^2) & 0 & -\lambda & 0 \\
0 & c_{44}^1/c_{66} & n/\eta & 0 \\
\lambda & -n/\eta & -d_3/\eta^2 - \rho\Omega^2/\rho^1 & -d_4\lambda/\eta \\
0 & 0 & -d_4\lambda/\eta & -\varepsilon_{22}n^2/(\varepsilon_{33}^1\eta^2) - d_5\lambda^2
\end{bmatrix},
$$

$$
\mathbf{D}_{21} = \begin{bmatrix}
c_{44}n^2/(c_{44}^1\eta^2) - d_6\lambda^2 - \rho\Omega^2/\rho^1 & -(c_{44}/c_{44}^1 - d_1)n\lambda/\eta & -c_{13}\lambda/c_{11} & 0 \\
-(c_{44}/c_{44}^1 - d_1)n\lambda/\eta & c_{44}\lambda^2/c_{44}^1 - d_3 n^2/\eta^2 - \rho\Omega^2/\rho^1 & c_{12}n/(c_{11}\eta) & 0 \\
c_{13}\lambda/c_{11} & -c_{12}n/(c_{11}\eta) & c_{44}^1/c_{11} & 0 \\
0 & 0 & 0 & -c_{55}\varepsilon_{33}^1/(c_{55}\varepsilon_{11} + e_{15}^2)
\end{bmatrix},
$$

$$
\mathbf{D}_{22} = \begin{bmatrix}
-1/\eta & 0 & d_1\lambda/\eta & e_{24}n^2/(\eta^2\sqrt{c_{44}^1\varepsilon_{33}^1}) + d_2\lambda^2 \\
0 & -2/\eta & -d_3 n/\eta^2 & -(e_{24}/\sqrt{c_{44}^1\varepsilon_{33}^1} + d_4)n\lambda/\eta \\
0 & 0 & -c_{12}/(c_{11}\eta) & \lambda e_{31}\sqrt{c_{44}^1}/(c_{11}\sqrt{\varepsilon_{33}^1}) \\
e_{15}\sqrt{c_{44}^1\varepsilon_{33}^1}/(c_{55}\varepsilon_{11} + e_{15}^2) & 0 & 0 & 0
\end{bmatrix}.
$$

For the present problem, the coefficient matrix $\mathbf{D}$ is not constant, making it difficult to get the solution to Eq. (6) directly. Here we employ the approximate laminate model, for which the cylinder is equally divided into p thin layers with the thickness (h/p) being very small. Thus, the coefficient matrix $\mathbf{D}$ can be assumed constant within each layer (denoted as $\mathbf{D}_j$ in the jth layer). In the following, the matrix $\mathbf{D}_j$ is assumed to take its value at each mid-plane, i.e. in Eq. (8), we have $c_{44} = c_{44}|_{\eta=1+(2j-1)h/(2pR)}$, etc. in the jth layer. Now within the layer, Eq. (6) can be solved as

$$
\mathbf{V}(\eta) = \exp[(\eta - \eta_{j0})\mathbf{D}_j]\mathbf{V}(\eta_{j0}) \quad (\eta_{j0} = 1 + (j-1)h/(pR) \leqslant \eta \leqslant \eta_{j1} = 1 + jh/(pR)). \tag{9}
$$

From Eq. (9), the following recurrence formulas are derived:

$$
\mathbf{V}(\eta_{j1}) = \exp[h\mathbf{D}_j/(pR)] \cdot \mathbf{V}(\eta_{j0}) \quad (j = 1, 2, \ldots, p). \tag{10}
$$

By virtue of the continuity conditions of state variables at each fictitious interface, one can obtain from Eq. (10),

$$\mathbf{V}^1 = \mathbf{T}\mathbf{V}^0, \tag{11}$$

where $\mathbf{T} = \prod_{j=p}^{1} \exp[h\mathbf{D}_j/(pR)]$, and $\mathbf{V}^0$ and $\mathbf{V}^1$ are the state vectors at the inner and outer cylindrical surfaces, respectively.

For a hollow cylinder completely filled with compressible, non-viscous fluid, the mechanical boundary conditions at the inner and outer cylindrical surfaces are known as (Chen et al., 1997; Chen and Ding, 1999)

$$\bar{\sigma}^0_{rr} = -\Omega^2 Q(1)\bar{u}^0_r \rho_{\mathrm{f}}/\rho^1, \quad \bar{\sigma}^0_{r\theta} = \bar{\sigma}^0_{rz} = \bar{\sigma}^1_{rr} = \bar{\sigma}^1_{r\theta} = \bar{\sigma}^1_{rz} = 0, \tag{12}$$

where ρ_{f} is the density of fluid ($\rho_{\mathrm{f}} = 0$ corresponds to the case in absence of fluid), and

$$Q(1) = \begin{cases} \dfrac{J_n(v)}{J_{n-1}(v) - J_{n+1}(v)} \cdot \dfrac{2}{v}, & v^2 > 0, \\ \dfrac{1}{n}, & v^2 = 0, \\ \dfrac{I_n(\tilde{v})}{I_{n-1}(\tilde{v}) + I_{n+1}(\tilde{v})} \cdot \dfrac{2}{\tilde{v}}, & v^2 = -\tilde{v}^2 < 0, \end{cases} \tag{13}$$

where $J_n(v)$ and $I_n(v)$ are Bessel function and modified Bessel function of the first kind, respectively, $v^2 = (c_{\mathrm{s}}^2/c_{\mathrm{f}}^2) \cdot \Omega^2 - \lambda^2$, in which c_{f} is the sound velocity in fluid and $c_{\mathrm{s}} = \sqrt{c^1_{44}/\rho^1}$ is the velocity of elastic wave in the solid.

In addition, there are two types of electrical conditions at the inner or outer cylindrical surfaces:

$$\text{Open circuit}: \ \overline{D}_r = 0; \quad \text{Closed circuit or shorted}: \ \overline{\Phi} = 0, \qquad \text{at } r = R \quad \text{or } r = R + h. \tag{14}$$

By applying the boundary conditions mentioned above in Eq. (11), we can acquire a system of linear equations. For example, in the case of both surfaces shorted, we can arrive at

$$\begin{Bmatrix} \bar{u}_z \\ \bar{u}_\phi \\ 0 \\ \overline{D}_r \\ 0 \\ 0 \\ \bar{u}_r \\ 0 \end{Bmatrix}^1 = \mathbf{T} \begin{Bmatrix} \bar{u}_z \\ \bar{u}_\phi \\ -\Omega^2 Q(1)\bar{u}_r \rho_{\mathrm{f}}/\rho^1 \\ \overline{D}_r \\ 0 \\ 0 \\ \bar{u}_r \\ 0 \end{Bmatrix}^0. \tag{15}$$

Considering the third, fifth, sixth, and eighth equations in Eq. (15), yields

$$\begin{Bmatrix} 0 \\ 0 \\ 0 \\ 0 \end{Bmatrix}^1 = \begin{bmatrix} T_{31} & T_{32} & T_{34} & T_{37} - T_{33}\Omega^2 Q(1)\rho_{\mathrm{f}}/\rho^1 \\ T_{51} & T_{52} & T_{54} & T_{57} - T_{53}\Omega^2 Q(1)\rho_{\mathrm{f}}/\rho^1 \\ T_{61} & T_{62} & T_{64} & T_{67} - T_{63}\Omega^2 Q(1)\rho_{\mathrm{f}}/\rho^1 \\ T_{81} & T_{82} & T_{84} & T_{87} - T_{83}\Omega^2 Q(1)\rho_{\mathrm{f}}/\rho^1 \end{bmatrix} \begin{Bmatrix} \bar{u}_z \\ \bar{u}_\phi \\ \overline{D}_r \\ \bar{u}_r \end{Bmatrix}^0, \tag{16}$$

where T_{ij} are elements of the matrix $\mathbf{T}$. Since Eq. (16) shall have non-trivial solution, the determinant of coefficients must vanish. Hence the frequency equation of a fluid-filled orthotropic FGPM hollow cylinder with two surfaces electrically shorted is obtained as

$$\begin{vmatrix} T_{31} & T_{32} & T_{34} & T_{37}-T_{33}\Omega^2 Q(1)\rho_{\mathrm{f}}/\rho^1 \\ T_{51} & T_{52} & T_{54} & T_{57}-T_{53}\Omega^2 Q(1)\rho_{\mathrm{f}}/\rho^1 \\ T_{61} & T_{62} & T_{64} & T_{67}-T_{63}\Omega^2 Q(1)\rho_{\mathrm{f}}/\rho^1 \\ T_{81} & T_{82} & T_{84} & T_{87}-T_{83}\Omega^2 Q(1)\rho_{\mathrm{f}}/\rho^1 \end{vmatrix} = 0. \tag{17}$$

For other combinations of electric boundary conditions, the frequency equations can be similarly obtained and omitted here.

5. Free vibration of a fluid-filled LPM hollow cylinder

Obviously, the above analysis can be applied to a fluid-filled N-layered piezoelectric hollow cylinder. In this case, we divide any layer into many sub-layers. Thus, within the mth layer, for example, we can obtain similarly

$$\mathbf{V}_m^1 = \mathbf{T}_m \mathbf{V}_m^0 \quad (m = 1, 2, \ldots, N), \tag{18}$$

where $\mathbf{T}_m = \prod_{j=p_m}^{1} \exp(h_m \mathbf{D}_j^m / p_m R)$, here p_m and h_m are the divided number and the thickness of the mth layer, respectively, and $\mathbf{V}_m^0$ and $\mathbf{V}_m^1$ are the state vectors at the inner and outer cylindrical surfaces of the mth layer, respectively.

Since the state variables are continuous at the interface between neighboring layers, we can derive from Eq. (18),

$$\mathbf{V}_N^1 = \mathbf{T}^* \mathbf{V}_1^0, \tag{19}$$

where $\mathbf{T}^* = \prod_{m=1}^{N} \mathbf{T}_m$.

The proceeding analysis then is identical to that for an FGPM hollow cylinder.

6. Numerical examples

Example 1 (*Free vibration of an infinite homogeneous piezoelectric hollow cylinder*). For an infinite piezoelectric hollow cylinder, the state vector $\mathbf{Y}$ can be expanded as

$$\mathbf{Y} = \begin{Bmatrix} u_z \\ u_\phi \\ \sigma_{rr} \\ D_r \\ \sigma_{zr} \\ \sigma_{r\phi} \\ u_r \\ \Phi \end{Bmatrix} = \sum_{n=0}^{\infty} \begin{Bmatrix} R\bar{u}_z(\eta)\cos(n\phi) \\ R\bar{u}_\phi(\eta)\sin(n\phi) \\ c_{44}^1 \bar{\sigma}_{rr}(\eta)\cos(n\phi) \\ \sqrt{c_{44}^1 \varepsilon_{33}^1}\,\overline{D}_r(\eta)\cos(n\phi) \\ c_{44}^1 \bar{\sigma}_{zr}(\eta)\cos(n\phi) \\ c_{44}^1 \bar{\sigma}_{r\phi}(\eta)\sin(n\phi) \\ R\bar{u}_r(\eta)\cos(n\phi) \\ R\sqrt{c_{44}^1/\varepsilon_{33}^1}\,\overline{\Phi}(\eta)\cos(n\phi) \end{Bmatrix} \mathrm{e}^{i(\chi\vartheta-\omega t)}, \tag{20}$$

where χ is the non-dimensional axial wave number and $\vartheta = z/R$. The followed analysis is similar to that described earlier in this paper and omitted here for brevity.

Table 1 presents the lowest non-dimensional natural frequencies ($\Omega = \omega R\sqrt{\rho^1/c_{44}^1}$) of a PZT-4 homogeneous hollow cylinder without internal fluid (empty cylinder, corresponding to $\rho_{\mathrm{f}} = 0$). The electric boundary condition is assumed to be shorted at both inner and outer cylindrical surfaces. The material constants of PZT-4 are listed in Table 2.

Table 1
Lowest natural frequencies of an infinite PZT-4 hollow cylinder with both surfaces shorted

	$\chi = 0.005$			$\chi = 0.500$			$\chi = 1.000$		
	$n = 0$	$n = 1$	$n = 2$	$n = 0$	$n = 1$	$n = 2$	$n = 0$	$n = 1$	$n = 2$
Paul and Venkatesan (1987)	Missed	Missed	1.09614	1.42886	Missed	1.30666	2.05896	Missed	1.74713
Ding et al. (1997a)	0.01582	0.00013	1.09611	1.43728	0.69679	1.29820	2.07361	1.65614	1.90402
Present	0.01588	0.00013	1.09448	1.44270	0.69744	1.24537	2.07745	1.65696	1.90435

Table 2
Material constants of two homogeneous piezoelectric materials

Property	c_{11}	c_{12}	c_{13}	c_{22}	c_{23}	c_{33}	c_{44}	c_{55}	c_{66}
Ψ^0 ($Ba_2NaNb_5O_{15}$)	23.9	10.4	5.0	24.7	5.2	13.5	6.5	6.6	7.6
Ψ^1 (PZT-4)	13.9	7.8	7.4	13.9	7.4	11.5	2.56	2.56	3.05
	e_{15}	e_{24}	e_{31}	e_{32}	e_{33}	ε_{11}	ε_{22}	ε_{33}	ρ
Ψ^0 ($Ba_2NaNb_5O_{15}$)	2.8	3.4	−0.4	−0.3	4.3	196	201	28	5.3
Ψ^1 (PZT-4)	12.7	12.7	−5.2	−5.2	15.1	650	650	560	7.5

Units: c_{ij} (10^{10} N/m^2), ε_{ij} (10^{-11} F/m), e_{ij} (C/m^2), ρ (kg/m^3).

As shown in Table 1, the comparison with Ding et al. (1997a) shows a reasonable agreement. The observation reported in Ding et al. (1997a) that some frequencies were missed by Paul and Venkatesan (1987) is validated here.

The dispersion curves of the non-dimensional wave phase velocity V ($= \Omega/\chi$) versus the non-dimensional axial wave number χ are plotted in Figs. 3 and 4 for $h/R = 0.05$ and 0.5, respectively. The cylinder is supposed to be shorted at both cylindrical surfaces. It is shown the dispersion curves are quite different for

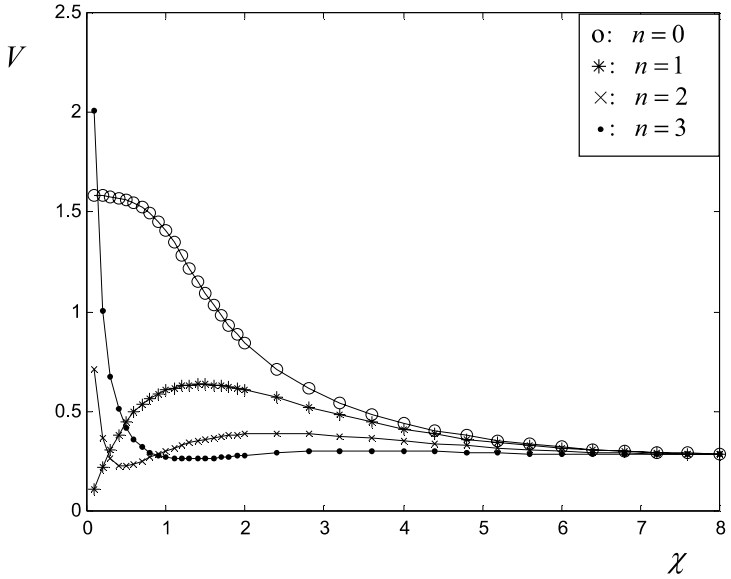

Fig. 3. Variation of non-dimensional wave phase velocity, V, with non-dimensional axial wave number, χ ($h/R = 0.05$).

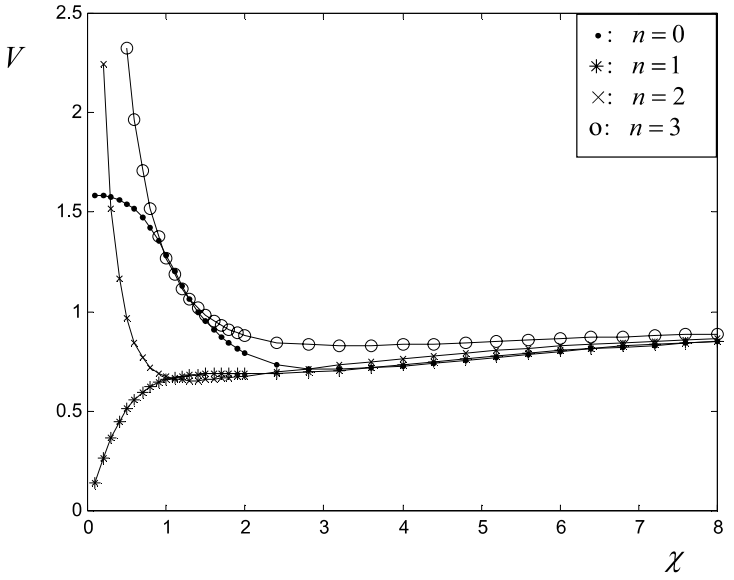

Fig. 4. Variation of non-dimensional wave phase velocity, V, with non-dimensional axial wave number, χ ($h/R = 0.5$).

different modes ($n = 0$ for longitudinal mode and $n > 0$ for flexural modes). They are also different for thin and thick piezoelectric cylinders, although all curves gradually become invariant with the further increase of χ. For example, for the mode number $n = 1$, V first increases and then decreases after a turning point when $h/R = 0.05$. When $h/R = 0.5$, however, it first increases, then decreases and finally increases with χ. This indicates that the observation for a thin shell could not be simply extended to for a thick shell.

Example 2 (*Free vibration of a fluid-filled FGPM hollow cylinder*). To analyze the free vibration behavior of FGPM hollow cylinder, the distributions of material properties must be assumed. There are several models in literature (Delale and Erdogan, 1988; Fuchiyama and Noda, 1995; Liu et al., 1999). Here we consider the following two typical models:

$$\text{Model I}: \ \Psi = \Psi^0(1-\beta) + \Psi^1\beta \quad \text{and} \quad \text{Model II}: \ \Psi = \Psi^0(\Psi^1/\Psi^0)^\beta,$$

where $\beta = [(r-R)/h]^\kappa$, Ψ represents an arbitrary material constant of the FGPM, while Ψ^0 and Ψ^1 are the corresponding ones for two homogeneous materials. The material constants of the two homogeneous piezoelectric materials considered in this paper, PZT-4 and $Ba_2NaNb_5O_{15}$ (Dieulesaint and Royer, 1980), are listed in Table 2. Fig. 5 shows the variations of the elastic constant c_{11} along the thickness direction for several values of κ, where solid and dotted lines correspond to Models I and II, respectively. It is seen that there is certain difference between Models I and II especially when κ is small. However, the variations of material constants of the two models along the thickness direction are very similar.

Fig. 6 displays the curves of the lowest non-dimensional natural frequency Ω versus the gradient parameter κ for different circumferential wave numbers (n). The thickness-to-inner radius ratio of the cylinder and the non-dimensional axial wave number are taken to be $h/R = 0.2$ and $\lambda = m\pi R/L = 3$, respectively. The filled fluid considered here is water with $\rho_f/\rho^1 = 0.13$ and $c_f/c_s = 0.27$. In addition, both surfaces of the cylinder are electrically shorted. In order to acquire a high numerical accuracy, we divide the cylinder into 60 layers. For the sake of comparison, the corresponding curves of the empty cylinder with other parameters identical are shown in Fig. 7.

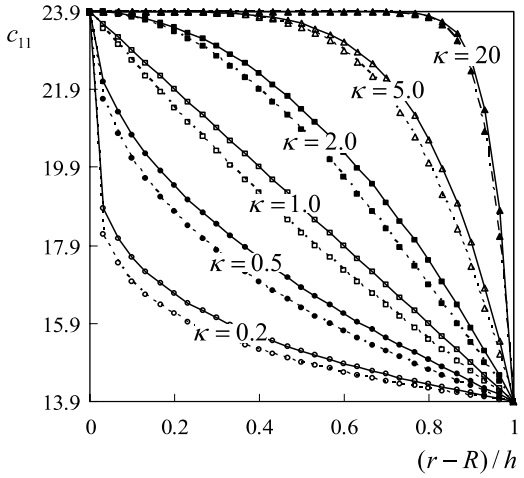

Fig. 5. Variation of elastic constant c_{11} (GPa) through thickness.

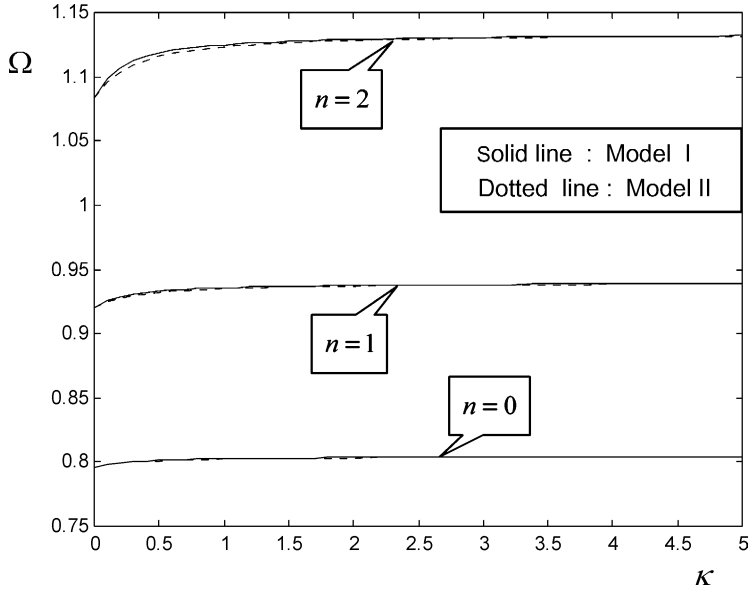

Fig. 6. Variation of lowest non-dimensional frequency Ω of fluid-filled cylinder with κ.

From the above two figures, we can see that the lowest natural frequency Ω of the fluid-filled cylinder is always lower than those of the empty cylinder, which is just due to the well-known "added mass effect" (Jain, 1974). This effect is obviously different for different wave modes. As we can see, in the empty case, the lowest natural frequency of the cylinder corresponds to the flexural mode $n = 2$, whereas it corresponds to the axisymmetric mode $n = 0$ for the fluid-filled cylinder. It is also interesting to note that the presence of fluid medium can reduce the impact of the gradient parameter κ on the frequency, which can be seen from the relatively gently varying curves in Fig. 6 as compared to those in Fig. 7. Furthermore, the difference between the frequency curves for Models I and II materials dwindles when the cylinder is filled with fluid.

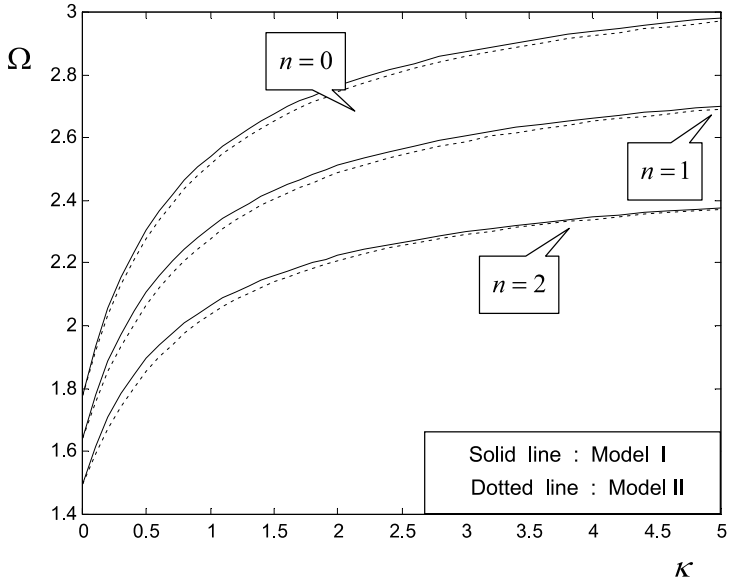

Fig. 7. Variation of lowest non-dimensional frequency Ω of empty cylinder with κ.

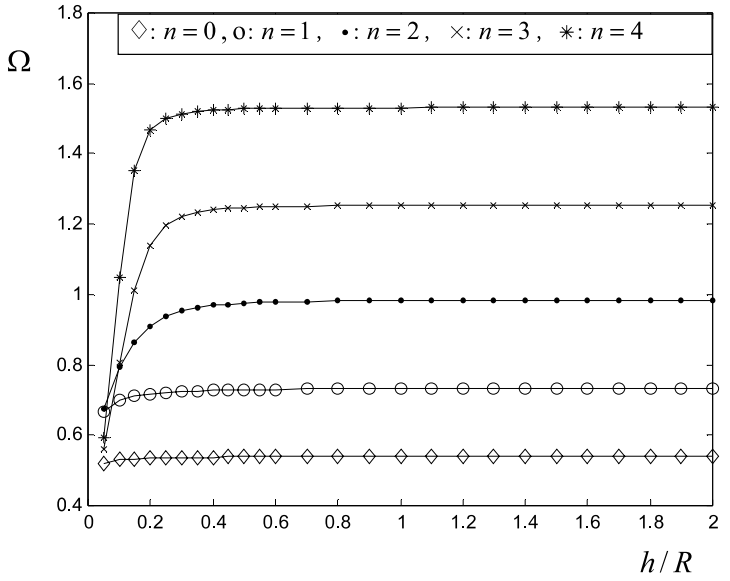

Fig. 8. Variation of lowest non-dimensional frequency Ω with h/R.

The effects of h/R and λ on Ω are depicted in Figs. 8 and 9, respectively. In Fig. 8, Model I material is employed with $\kappa = 1$ and $\lambda = 2$, while Model II material is assumed to obtain the results in Fig. 9 with $\kappa = 2$ and $h/R = 1$. The filled fluid is still water. Also, the number of layers is $p = 60$, which can assure the relative error of these results within 10^{-4}.

It is shown that the non-dimensional frequency Ω increases rapidly with h/R at the initial stage, but then it keeps almost invariant. This implies that the frequency of the cylinder with $h/R = 2.0$, for example, will

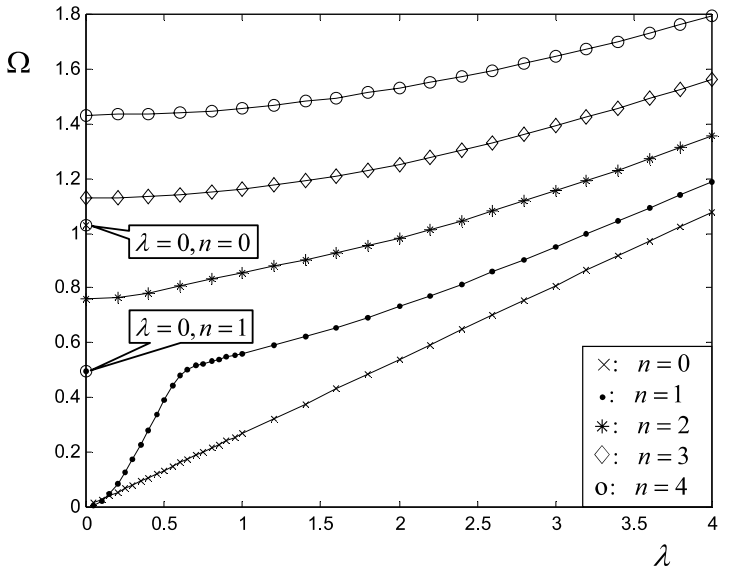

Fig. 9. Variation of lowest non-dimensional natural frequency Ω with λ.

be very close to that of an infinite solid with a cylinder cavity of radius R. As expected (Mirsky, 1964), Fig. 9 shows that the frequency increases with the non-dimensional axial wave number λ. The curve for $n = 1$ seems very different from the others; however, this is not always the case when the parameters of the filled fluid or the geometric size of the cylinder are changed. The results are not presented here for brevity, but the reader is referred to Ding et al. (1997a) for similar results of a homogeneous cylinder. In the calculation, we also find that for the purely axial vibration ($m = 0$), the frequencies corresponding to $n = 0, 1$ are quite different from those for the non-axial vibration ($\lambda \neq 0$), as shown in Fig. 9.

Example 3 (*Free vibration of a fluid-filled LPM hollow cylinder*). Consider a three-layered LPM hollow cylinder, whose inner and outer layers are made of PZT-4, while the mid-layer is $Ba_2NaNb_5O_{15}$. The geometry of the layers is $h_1 : h_2 : h_3 : R = 0.3 : 0.4 : 0.3 : 1$. For the sake of precision, each layer is divided into 20 sub-layers.

Figs. 10 and 11 display the curves of the lowest non-dimensional frequency Ω versus fluid parameters ρ_f/ρ^1 and c_f/c_s, respectively, with different combinations of electrical boundary conditions at the inner and outer cylindrical surfaces. The non-dimensional axial wave number in both figures is taken to be $\lambda = 2$. In addition, results in Fig. 10 are obtained for $c_f/c_s = 0.27$, while Fig. 11 is for $\rho_f/\rho^1 = 0.13$.

As shown in Fig. 10, the frequency almost keeps invariant with the increase of ρ_f/ρ^1, while it increases with c_f/c_s significantly as shown in Fig. 11. This indicates that the natural frequency is more sensitive to c_f/c_s than to ρ_f/ρ^1. This property should be very important for the design of fluid-filled cylinders. It is noted here that totally four types of electric conditions (i.e. both surfaces shorted, inner shorted and outer open, inner open and outer shorted, and both open) are considered and the results are simultaneously given in Figs. 10 and 11. The curves for different electrical boundary conditions in Fig. 10 are wrapped together indicating that the electric conditions have little influence on the lowest frequency. However, with the increase of the velocity ratio, the frequencies will be different for different electric boundary conditions especially for $n = 4$, as shown in Fig. 11, where the curves are not specified by the respective electric conditions but are shown just for illustration.

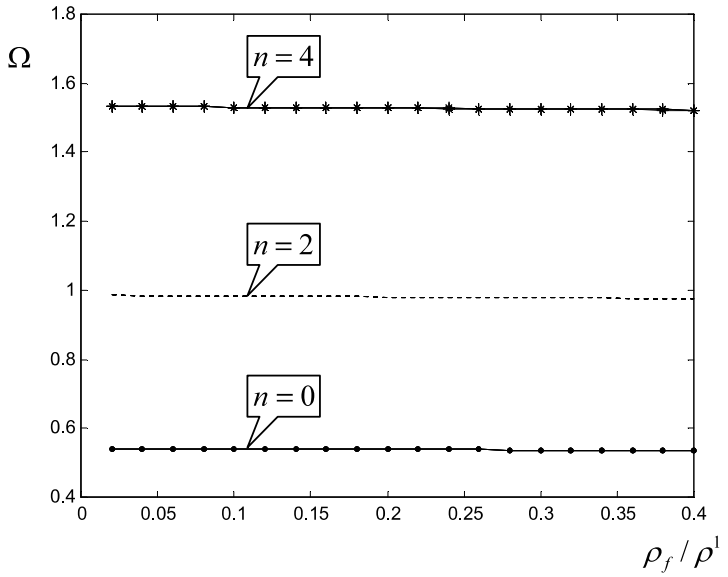

Fig. 10. Variation of lowest non-dimensional natural frequency Ω with ρ_f/ρ^1.

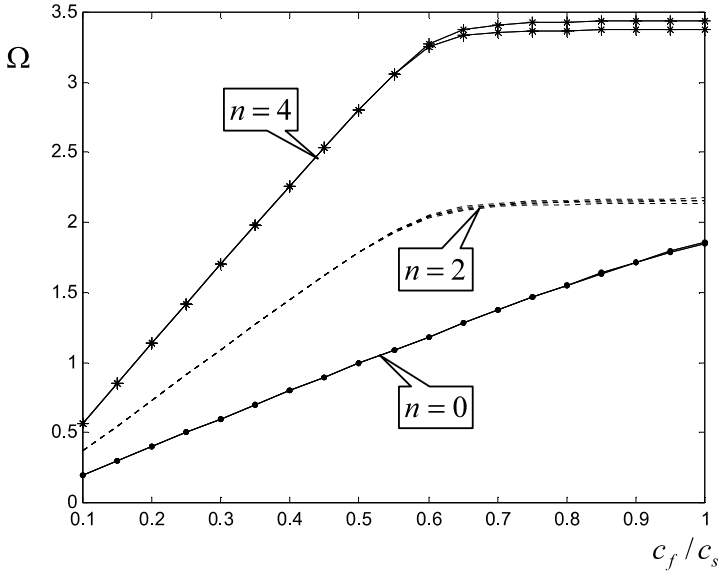

Fig. 11. Variation of lowest non-dimensional natural frequency Ω with c_f/c_s.

7. Conclusions

In this paper, the coupled free vibration of a functionally graded piezoelectric hollow cylinder filled with a non-viscous, compressible fluid medium is investigated. Owing to the disadvantage characterized by the

conventional shell theories in modeling the FGM structures, the state-space method is employed, which is completely based on the three-dimensional theory of piezoelasticity. Because of the curvilinear coordinates and the inhomogeneity of material, the resulting state equation is with variable coefficients, of which the solution is difficult to obtain directly. For the sake of simplicity, an approximate laminate model is adopted to transform the state equation to the one with constant coefficients whose solution can be obtained using matrix theory.

Numerical calculations are performed. Comparison with existent results for an infinite empty piezoelectric hollow cylinder shows a good agreement, validating the correctness and effectiveness of the present method. Numerical results also show that frequency of the cylinder can differ significantly in the presence of a fluid medium. Thus when a structure is contacting with ambient media, the coupling effect should be taken into account to give an accurate prediction. Two different models considering the functionally graded property of material are adopted in the paper. Results show that the material design based on the FGM concept can play an important role in practical engineering.

Since no assumptions are introduced on the deformations or stress fields in the cylinder, the results presented in this paper can serve as benchmarks for clarifying the reliability of various approximate shell theories or numerical methods. The only approximation is introduced when the laminate model is employed. However, when the number of layers increases, the solution of the model will gradually approach the exact one of the original cylinder. One significant merit of the model is that it allows one to deal with arbitrary variations of the material constants. The variation of one material constant can also differ from that of the other one. Combing with the state-space method, the numerical efficiency is very prominent.

Acknowledgements

This work was supported by the National Natural Science Foundation of China (No. 10002016). The authors also would like to thank the anonymous reviewers for their constructive comments on an earlier version of the paper.

Appendix A

The operator matrix $\mathbf{M}$ in Eq. (4) is defined as follows:

$$\mathbf{M} = \begin{bmatrix} \mathbf{M}_1 & \mathbf{M}_2 \\ \mathbf{M}_3 & \mathbf{M}_4 \end{bmatrix},$$

$$\mathbf{M}_1 = \begin{bmatrix} 0 & 0 & 0 & \frac{e_{15}}{\alpha} \\ 0 & \frac{1}{r} & 0 & 0 \\ \frac{k_2}{r}\frac{\partial}{\partial z} & \frac{k_1}{r^2}\frac{\partial}{\partial \phi} & \left(\frac{c_{12}}{c_{11}} - 1\right)\frac{1}{r} & 0 \\ -\frac{e_{24}}{r^2}\frac{\partial^2}{\partial \phi^2} - k_5\frac{\partial^2}{\partial z^2} & -\frac{e_{24}+k_3}{r}\frac{\partial^2}{\partial \phi \partial z} & -\frac{e_{31}}{c_{11}}\frac{\partial}{\partial z} & -\frac{1}{r} \end{bmatrix},$$

$$\mathbf{M}_2 = \begin{bmatrix} \frac{\varepsilon_{11}}{\alpha} & 0 & -\frac{\partial}{\partial z} & 0 \\ 0 & \frac{1}{c_{66}} & -\frac{1}{r}\frac{\partial}{\partial \phi} & 0 \\ -\frac{\partial}{\partial z} & -\frac{1}{r}\frac{\partial}{\partial \phi} & \rho\frac{\partial^2}{\partial t^2}+\frac{k_1}{r^2} & \frac{k_3}{r}\frac{\partial}{\partial z} \\ 0 & 0 & -\frac{k_3}{r}\frac{\partial}{\partial z} & \frac{\varepsilon_{22}}{r^2}\frac{\partial^2}{\partial \phi^2}+k_6\frac{\partial^2}{\partial z^2} \end{bmatrix},$$

$$\mathbf{M}_3 = \begin{bmatrix} \rho\frac{\partial^2}{\partial t^2}-\frac{c_{44}}{r^2}\frac{\partial^2}{\partial \phi^2}-k_4\frac{\partial^2}{\partial z^2} & -\frac{c_{44}+k_2}{r}\frac{\partial^2}{\partial \phi \partial z} & -\frac{c_{13}}{c_{11}}\frac{\partial}{\partial z} & 0 \\ -\frac{c_{44}+k_2}{r}\frac{\partial^2}{\partial \phi \partial z} & \rho\frac{\partial^2}{\partial t^2}-\frac{k_1}{r^2}\frac{\partial^2}{\partial \phi^2}-c_{44}\frac{\partial^2}{\partial z^2} & -\frac{c_{12}}{c_{11}}\frac{1}{r}\frac{\partial}{\partial \phi} & 0 \\ -\frac{c_{13}}{c_{11}}\frac{\partial}{\partial z} & -\frac{c_{12}}{c_{11}}\frac{1}{r}\frac{\partial}{\partial \phi} & \frac{1}{c_{11}} & 0 \\ 0 & 0 & 0 & -\frac{c_{55}}{\alpha} \end{bmatrix},$$

$$\mathbf{M}_4 = \begin{bmatrix} -\frac{1}{r} & 0 & -\frac{k_2}{r}\frac{\partial}{\partial z} & -\frac{e_{24}}{r^2}\frac{\partial^2}{\partial \phi^2}-k_5\frac{\partial^2}{\partial z^2} \\ 0 & -\frac{2}{r} & -\frac{k_1}{r^2}\frac{\partial}{\partial \phi} & -\frac{e_{24}+k_3}{r}\frac{\partial^2}{\partial \phi \partial z} \\ 0 & 0 & -\frac{c_{12}}{c_{11}}\frac{1}{r} & -\frac{e_{31}}{c_{11}}\frac{\partial}{\partial z} \\ \frac{e_{15}}{\alpha} & 0 & 0 & 0 \end{bmatrix},$$

where

$$k_1 = c_{22} - c_{12}^2/c_{11}, \quad k_2 = c_{23} - c_{12}c_{13}/c_{11}, \quad k_3 = e_{32} - c_{12}e_{31}/c_{11}, \quad k_4 = c_{33} - c_{13}^2/c_{11},$$
$$k_5 = e_{33} - c_{13}e_{31}/c_{11}, \quad k_6 = \varepsilon_{33} + e_{31}^2/c_{11}, \quad \alpha = c_{55}\varepsilon_{11} + e_{15}^2.$$

References

Babaev, A.E., But, L.M., Savin, V.G., 1990. Transient vibrations of a thin-walled cylindrical piezoelectric vibrator driven by a nonaxisymmetric electric sign in a liquid. Soviet Applied Mechanics 26, 1167–1174.

Babaev, A.E., Savin, V.G., 1988. Nonsteady hydroelasticity of a system of coaxial piezoceramic cylindrical shells during electrical excitation. Soviet Applied Mechanics 24, 1069–1074.

Ballato, J., Schwartz, R., Ballato, A., 2001. Network formalism for modeling functionally gradient piezoelectric plates and stacks and simulations of RAINBOW ceramic actuators. IEEE Transactions on Ultrasonics, Ferroelectrics and Frequency Control 48, 462–476.

Bugdayci, N., Bogy, D.B., Talke, F.E., 1983. Axisymmetric motion of radially polarized piezoelectric cylinders used in ink jet printing. IBM Journal of Research and Development 27, 171–180.

Chen, C.Q., Shen, Y.P., 1998. Three-dimensional analysis for the free vibration of finite-length orthotropic circular cylindrical shells. Journal of Vibration & Acoustics 120, 194–198.

Chen, W.Q., Ding, H.J., 1999. Natural frequencies of fluid-filled transversely isotropic cylindrical shells. International Journal of Mechanical Sciences 41, 677–684.

Chen, W.Q., Ding, H.J., 2000. Bending of functionally graded piezoelectric rectangular plates. Acta Mechanica Solida Sinica 13, 312–319.

Chen, W.Q., Ding, H.J., 2001. Free vibration of multi-layered spherical isotropic hollow sphere. International Journal of Mechanical Sciences 43, 667–680.

Chen, W.Q., Ding, H.J., 2002. On free vibration of a functionally graded piezoelectric rectangular plate. Acta Mechanica 153, 207–216.

Chen, W.Q., Ding, H.J., Guo, Y.M., Yang, Q.D., 1997. Free vibrations of fluid-filled orthotropic cylindrical shells. Journal of Engineering Mechanics 123, 1130–1133.

Chen, W.Q., Ding, H.J., Xu, R.Q., 2001. Three dimensional free vibration analysis of a fluid-filled piezoceramic hollow sphere. Computers & Structures 79, 653–663.

Delale, F., Erdogan, F., 1988. On the mechanical modeling of the interfacial region in bonded half-planes. Journal of Applied Mechanics 55, 317–324.

Dieulesaint, E., Royer, D., 1980. Elastic Waves in Solids. John Wiley, New York.

Ding, H.J., Chen, W.Q., 2001. Three Dimensional Problems of Piezoelasticity. Nova Science Publishers, New York.

Ding, H.J., Chen, W.Q., Guo, Y.M., Yang, Q.D., 1997a. Free vibrations of piezoelectric cylindrical shells filled with compressible fluid. International Journal of Solids and Structures 34, 2025–2034.

Ding, H.J. et al., 1997b. Elasticity of Transversely Isotropic Materials. Zhejiang University Press, Hangzhou (in Chinese).

Fan, J.R., 1996. Exact Theory of Strongly Thick Laminated Plates and Shells. Science Press, Beijing (in Chinese).

Fan, J.R., Zhang, J.Y., 1992. Analytical solution for thick, doubly curved, laminated shells. Journal of Engineering Mechanics 118, 1338–1356.

Fuchiyama, T., Noda, N., 1995. Analysis of thermal stress in a plate of functionally gradient material. JSAE Review 16, 263–268.

Galassi, C., Dinescu, M., Uchino, K., Sayer, M. (Eds.), 2000. Piezoelectric Materials: Advances in Science, Technology and Applications. Kluwer, Dordrecht.

Grosh, K., Lin, Y., Silva, E.C., Kikuchi, N., 1998. Design of fluid-loaded piezoelectric transducers for acoustic power considerations. In: Varadan, V.V. (Ed.), SPIE Proceedings. Smart Structures and Materials 1998: Mathematics and Control in Smart Structures, vol. 3323, pp. 20–30.

Han, X., Liu, G.R., Xi, Z.C., Lam, K.Y., 2001. Transient waves in a functionally graded cylinder. International Journal of Solids and Structures 38, 3021–3037.

Jain, R.K., 1974. Vibration of fluid-filled, orthotropic cylindrical shells. Journal of Sound and Vibration 37, 379–388.

Junger, M.C., Mass, C., 1952. Vibrations of elastic shells in a fluid medium and the associated radiation of sound. Journal of Applied Mechanics 19, 439–445.

Kapuria, S., Sengupta, S., Dumir, P.C., 1997. Three-dimensional solution for simply-supported piezoelectric cylindrical shell for axisymmetric load. Computer Methods in Applied Mechanics and Engineering 140, 139–155.

Li, C.Y., Weng, G.J., 2002. Antiplane crack problem in functionally graded piezoelectric materials. Journal of Applied Mechanics 69, 481–488.

Liu, G.R., Tani, J., 1991. Characteristics of wave propagation in functionally gradient piezoelectric material plates and its response analysis, Part 1 and Part 2. Transactions of the Japan Society of Mechanical Engineers 57A, 2122–2133 (in Japanese).

Liu, G.R., Tani, J., 1992. SH surface waves in functionally gradient piezoelectric material plates. Transactions of the Japan Society of Mechanical Engineers 58A, 504–507 (in Japanese).

Liu, G.R., Han, X., Lam, K.Y., 1999. Stress waves in functionally gradient materials and its use for material characterization. Composites Part B: Engineering 30, 383–394.

Loy, C.T., Lam, K.Y., Reddy, J.N., 1999. Vibration of functionally graded cylindrical shells. International Journal of Mechanical Sciences 41, 309–324.

Mirsky, I., 1964. Vibrations of orthotropic, thick, cylindrical shells. Journal of the Acoustical Society of America 36, 41–51.

Morita, T., Kurosawa, M., Higuchi, T., 1995. An ultrasonic micromotor using a bending cylindrical transducer based on PZT thin film. Sensors and Actuators A 50, 75–80.

Moulson, A.J., Herbert, J.M., 1990. Electroceramics: Materials, Properties and Applications. Chapman and Hall, New York.

Paul, H.S., Venkatesan, M., 1987. Vibrations of a hollow circular cylinder of piezoelectric ceramics. Journal of the Acoustical Society of America 82, 952–956.

Pradhan, S.C., Loy, C.T., Lam, K.Y., Reddy, J.N., 2000. Vibration characteristics of functionally graded cylindrical shells under various boundary conditions. Applied Acoustics 61, 111–129.

Rogacheva, N., 1994. The Theory of Piezoelectric Shells and Plates. CRC Press, Boca Raton, LA.

Saha, S., Williams, P.A., 1996. The electrical and dielectric properties of human bone tissue and their relationship with density and bone mineral content. Annals of Biomedical Engineering 24, 222–233.

Sakamura, J., Yamada, K., Nakamura, K., 2000. Equivalent network analysis of functionally graded piezoelectric transducers. Japanese Journal of Applied Physics (Part 1) 39, 3150–3151.

Shulga, N.A., Melnik, S.I., 1996. Energy analysis of axisymmetric wave propagation in a hollow liquid-containing piezoelectric cylinder. International Applied Mechanics 32, 81–88.

Soldatos, K.P., Hadhgeorgiou, V.P., 1990. Three-dimensional solution of the free vibration problem of homogeneous isotropic cylindrical shells and plates. Journal of Sound and Vibration 137, 369–384.

Takagi, K., Li, J.F., Yokoyama, S., Watanabe, R., Almajid, A., Taya, M., 2002. Design and fabrication of functionally graded PZT/Pt piezoelectric bimorph actuator. Science and Technology of Advanced Materials 3, 217–224.

Takahashi, S., Miyamoto, N., Ichinose, N., 2002. Functionally gradient piezoelectric ceramics for ultrasonic transducers. Japanese Journal of Applied Physics (Part 1) 41, 7103–7107.

Tanigawa, Y., 1995. Some basic thermoelastic problems for nonhomogeneous structural materials. Applied Mechanics Reviews 48, 287–300.

Tarn, J.Q., 2001. Exact solutions for functionally graded anisotropic cylinders subjected to thermal and mechanical loads. International Journal of Solids and Structures 38, 8189–8206.

Tzou, H.S., Anderson, G.L. (Eds.), 1992. Intelligent Structural Systems. Kluwer, Dordrecht.

Uchino, K., 1996. Piezoelectric Actuators and Ultrasonic Motors. Kluwer, Boston.

Wang, Q., 2001. Wave propagation in a piezoelectric coupled cylindrical membrane shell. International Journal of Solids and Structures 38, 8207–8218.

Wu, C.C.M., Kahn, M., Moy, W., 1996. Piezoelectric ceramics with functional gradients: a new application in material design. Journal of American Ceramic Society 79, 809–812.

Wu, X.H., Chen, C.Q., Shen, Y.P., Tian, X.G., 2002. A high order theory for functionally graded piezoelectric shells. International Journal of Solids and Structures 39, 5325–5344.

Wu, X.H., Shen, Y.P., Chen, C.Q., 2003. An exact solution for functionally graded piezothermoelastic cylindrical shell as sensors and actuators. Materials Letters 57, 3532–3542.

Xu, K.M., Noor, A.K., 1996. Three-dimensional analytical solutions for coupled thermoelectroelastic response of multi-layered cylindrical shells. AIAA Journal 34, 802–812.

Xu, K.M., Noor, A.K., Burton, W.S., 1997. 3D solutions for free vibration of initially stressed thermoelectroelastic multilayered cylinders. Journal of Engineering Mechanics 123, 45–51.

Yamada, K., Yamazaki, D., Nakamura, K., 2001. A functionally graded piezoelectric material created by an internal temperature gradient (Part 1). Japanese Journal of Applied Physics 40, L49–L52.

Yamanouchi, M., Koizumi, M., Hirai, T., Shiota, I., 1990. In: Proceeding of the First International Symposium on Functionally Gradient Materials, Japan.

Zhang, X.M., Liu, G.R., Lam, K.Y., 2001. Coupled vibration analysis of fluid-filled cylindrical shells using the wave propagation approach. Applied Acoustics 62, 229–243.

Zhou, J.P., Li, D.K., Li, A.L., 1999. Analysis of laminated piezoelectric cylindrical shells. Acta Mechanica Sinica 15, 145–154.

Zhu, X., Wang, Q., Meng, Z., 1995. A functionally gradient piezoelectric actuator prepared by power metallurgical process in PNN–PZ–PT system. Journal of Material Science Letter 14, 516–518.